Materials Science and Engineering B 279 (2022) 115674

Contents lists available at ScienceDirect

Materials Science & Engineering B

journal homepage: www.elsevier.com/locate/mseb

# Synthesis and analysis of low field high magnetostrictive Ni-Co ferrite for magneto-electric energy harvesting applications

P. Sowjanya [a,d], N. Pavan Kumar [b], Arout Chelvane [c], M.V. Ramana Reddy [a,e,*]

[a] Department of Physics, Osmania University, Hyderabad, Telangana, India
[b] Department of Sciences and Humanities, Matrusri Engineering College, Hyderabad, Telangana, India
[c] Advanced Magnetics Group, Defence Metallurgical Research Laboratory, Kanchanbagh, Hyderabad, Telangana, India
[d] Department of Physics, Government Degree College for Women, Gajwel, Telangana, India
[e] Department of Physics, Jawaharlal Nehru Technological University, Kukatpally, Hyderabad, Telangana, India

ARTICLE INFO

*Keywords:*
Magnetostriction
Ferrites
Ni-Co ferrites

ABSTRACT

Low field high magnetostrictive cobalt substituted nickel ferrites with composition $Ni_{1-x}Co_xFe_2O_4$ (x = 0, 0.25, 0.5, 0.75 and 1) were synthesized by sol gel technique. The formation of cubic spinel structure of samples was confirmed by X-ray diffraction. Surface morphology and optical properties were studied by using scanning electron microscopy and Differential Reflectance spectroscopy. The systematic change in the Metal-Oxygen (M−O) bands with Co substitution in nickel ferrite samples was observed in Fourier Transform Infrared spectra. With Co substitution remanance and coercivity values were increased and Curie temperature values were decreased systematically. The magnetostriction was found to increase with the substitution of Co from 10 ppm to a maximum value of about 200 ppm. $Ni_{0.5}Co_{0.5}Fe_2O_4$ showed magnetostriction of ~−63 ppm at 1500 Oe and ~−85 ppm at 2000 Oe and strain sensitivity value $1.74x10^{-9}A^{-1}m$ at 1500 Oe.

## 1. Introduction

Nowadays there is a great attention on magnetostrictive materials because of their wide usage in technological applications of magneto electric energy harvesting. A highly magnetostrictive material is an essential part of magneto electric (ME) materials. In magnetostrictive materials, magnetic domains rotate under external mechanical stress and expand proportionally to the load, modifying the magnetic properties due to inverse magnetostriction (Villari effect). Magnetostrictive devices exhibit energy harvesting potential by inducing current in a wire coiled around the material due to a change in magnetic flux [1].

Magnetostrictive ferrites are widely useful in advanced magneto mechanical stress sensors, actuators and torque sensors [2]. Oxide based magnetostrictive materials are suitable for various applications due to the low cost, high mechanical stability, better coupling coefficient, low thermal conductivity, high electrical resistance, and excellent corrosion resistance. Among many $AB_2O_4$ spinel ferrites, nickel ferrite is a soft magnetic material with low magnetic coercivity, low saturation magnetization and hysteresis loss. Cobalt ferrite is a hard magnetic material with relatively high coercivity and saturation magnetization. Because of good physical and chemical stability, major research work has been done on these spinel ferrites. Pure as well as substituted nickel ferrites have been extensively investigated because of their wide applications [3-8]. The general chemical formula of spinel structure is given by $(A_xB_{1-x})O[A_{1-x}B_{1+x}]O_3$ where cations inside the parenthesis "()" are indicated to be in tetrahedral sites and those inside the bracket "[ ]" are in octahedral sites. Here 'x' varies from 0 to 1 depending on the materials; When x = 1formula will be $A^{+2}[B^{+3}{}_2]O^{-2}{}_4$ and the material is called normal spinel. When x = 0 formula changes as $B^{+3}[A^{+2}B^{+3}]O^{-2}{}_4$ and the material is called inverse spinel. When 0 < x < 1 the material is called mixed spinel [9].The spinel structure of Co/Ni ferrites consists of a cubic close packed lattice of 32 oxygen atoms with the metal ions distributed in two different sub-lattices: 8 tetrahedral $Ni^{+2}$ or $Co^{+2}$ (A-sites) and 16 octahedral $Fe^{+3}$ (B-sites). The inverse spinel structure is characterized by 8 $Ni^{+2}$ or $Co^{+2}$ and 8 $Fe^{+3}$cations occupying half of the octahedral sites and 8 $Fe^{+3}$ ions occupying tetrahedral sites. In the mixed spinel structure, the number of $Fe^{+3}$ ions in octahedral sites increase, while that of the $Fe^{+3}$ ions in tetrahedral sites decrease due to the presence of divalent ions ($Ni^{+2}$, $Co^{+2}$) in tetrahedral sites.

It is well known that nickel ferrite has an inverse spinel structure with $Ni^{+2}$ ions at octahedral [B] sites and $Fe^{+3}$ ions equally distributed at tetrahedral (A) and octahedral [B] sites and cobalt ferrite usually

* Corresponding author.
*E-mail address:* muskuramana@gmail.com (M.V.R. Reddy).

https://doi.org/10.1016/j.mseb.2022.115674
Received 6 June 2021; Received in revised form 30 January 2022; Accepted 24 February 2022
Available online 4 March 2022

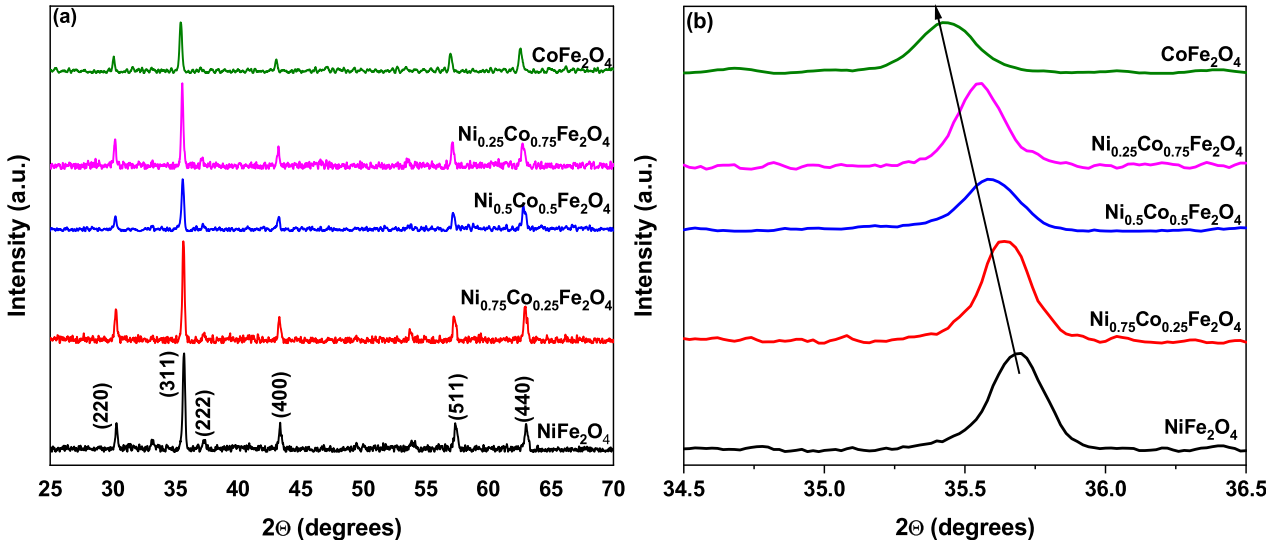


**Fig. 1.** (a) XRD patterns of all Co substituted Ni ferrites, (b) Close view of (311) peak shift with Co concentration.

exhibits a mixed spinel structure which is an intermediate stage of inversion where both sites contain a fraction of $Co^{+2}$ and $Fe^{+3}$ depending on synthesis and annealing [10]. Nickel ferrite has a magnetostriction value −10 ppm and gets saturated around 2000 Oe, and cobalt ferrite has −120 ppm around 5000 Oe.[11,12].

Influence of cobalt on structural, electrical and magnetic properties of nickel ferrites $Ni_{1-x}Co_xFe_2O_4$ with different compositions were reported [6,13–23] by different preparation techniques. Adding hard magnetic material like cobalt ferrite to soft magnetic material of nickel ferrite makes it useful for many different applications like data storage, information delivery devices, microwave absorption material etc. With Co substitution in $NiFe_2O_4$, Co prefers to occupy octahedral site hence redistribution of cations takes place. In this redistribution process, $Ni^{+2}$ ions migrate from octahedral to tetrahedral sites and some $Fe^{3+}$ ions also migrate from tetrahedral to octahedral sites [24]. This type of cationic rearrangement leads to induced intrinsic strain as a result of atomic rearrangements and differences in ionic radii. So, many defects get created within the nanocrystals, which can influence the optical, magnetic and magnetostriction properties [25]. Also, choosing proper magnetic probe material for designing optical fiber based magnetic field sensors is a challenging task where optical fiber coated with ferrite nanoparticle has found wide application for sensing of small magnetic fields [26].

Structural, magnetic, electrical and optical studies of Ni-Co nano ferrite with composition $Ni_{1-x}Co_xFe_2O_4$ where x = 0, 0.25, 0.5, 0.75 and 1 [25,27–34] were discussed earlier by few researchers. Perusal of literature indicates that there was only one report on magnetostrictive properties of nanocrystalline nickel substituted cobalt ferrite [20] in which very low magnetostriction values were reported at low magnetic fields.

For better energy harvesting, preparation and study of tunable magnetostrictive ferrites having high strain ($\lambda$) values even at low magnetic fields along with good magneto mechanical coupling factor is the aim of this study. Also for stress and torque sensor applications, the maximum strain derivative $(\frac{d\lambda}{dH})_{max}$ is more important along with saturation magnetostriction [35]. Hence a systematic study of tunability of magnetostriction for Ni-Co ferrite along with $NiFe_2O_4$, $CoFe_2O_4$ has been carried out.

In the present study sol–gel method was used for the preparation of Ni-Co ferrites. This is a simple and cost effective process to prepare materials with metal oxides and can control the doping process as compared to other preparation techniques. From sol–gel process, a high degree of homogeneity and purity can be obtained. In addition, required quantities of dopants can be introduced into the chemical solution and incorporated into the final product. The distinguished fact in sol–gel method is that the desired metal oxide materials can be synthesized at lower temperatures. In this work, ferrites with the compositional formula $Ni_{1-x}Co_xFe_2O_4$ (x = 0, 0.25, 0.5, 0.75 and 1) are synthesized and their structural, optical and magnetic properties along with magnetostrictive properties are presented and discussed here.

## 2. Experimental details

The cobalt substituted nickel ferrites with the compositional formula $Ni_{1-x}Co_xFe_2O_4$ (x = 0, 0.25, 0.5, 0.75 and 1) are synthesized by sol–gel technique. The starting materials $Ni(NO_3)_2{\cdot}6H_2O$, $Co(NO_3)_2{\cdot}6H_2O$, $Fe(NO_3)_3{\cdot}9H_2O$ were dissolved in double distilled water separately. Later these solutions were mixed and stirred together for 30mins to get the homogeneous solution. Later, citric acid has been added to the ratio of 1:1 to the metal ions. Then the pH of the solution was adjusted to 6–7 by adding ammonia solution and heated at 80°C until it reaches one-third of the solution. Then ethylene glycol was added as a gelating reagent and eutectic solvent during the process. The gelation time was approximately 20 hrs at 120°C. After drying, powders were pre-heated in Bunsen burner and later calcined at 800 °C in a furnace under air atmosphere. Finally, the prepared powders were made into two types of disk shaped pellets of 10 mm diameter with the aid of pelletizer and sintered at 1200 °C for 4hrs. For magnetostriction 15 mm thickness disks were used and for remaining characterizations approximately 1 mm thickness disks were used.

The prepared sintered ferrite powder samples were characterized by powder X-ray diffraction using Rigaku Mini Flex 600 with Cu $K_\alpha$ radiation. Optical studies were done by UV DRS method in the wavelength region of 200–900 nm. FTIR transmission spectra were recorded in the range 4000–200 $cm^{-1}$. The prepared sintered pellets were used to record the microstructural features by using an EVO18 scanning electron microscope (SEM). Magnetic properties were studied on the Vibrating Sample Magnetometer of model No.EV9 ADE, USA. Room temperature magnetostriction measurement was carried out by using a strain indicator.

## 3. Results and discussion

### 3.1. XRD

The XRD patterns for cobalt substituted nickel ferrite powders were

**Table 1**
The lattice parameter, crystallite size, volume, X-ray density, hopping lengths of A and B sites, Grain size (from SEM) for all Co substituted Ni ferrites depending on the composition.

| Sample name | Lattice parameter a(Å) | Crystallite size D (nm) | Volume $a^3$(Å $^3$) | X-ray density (gm/$cm^3$) | $L_A$ (Å) | $L_B$(Å) | Grain size (μm) |
|---|---|---|---|---|---|---|---|
| $NiFe_2O_4$ | 8.335 | 67.6 | 578.984 | 5.377 | 3.609 | 2.947 | 1.43 |
| $Ni_{0.75}Co_{0.25}Fe_2O_4$ | 8.348 | 72.1 | 581.818 | 5.352 | 3.615 | 2.952 | 1.6 |
| $Ni_{0.5}Co_{0.5}Fe_2O_4$ | 8.362 | 65.8 | 584.671 | 5.327 | 3.621 | 2.956 | 1.78 |
| $Ni_{0.25}Co_{0.75}Fe_2O_4$ | 8.366 | 75.2 | 585.628 | 5.32 | 3.623 | 2.958 | 3.1 |
| $CoFe_2O_4$ | 8.398 | 64.5 | 592.373 | 5.261 | 3.637 | 2.969 | 1.9 |

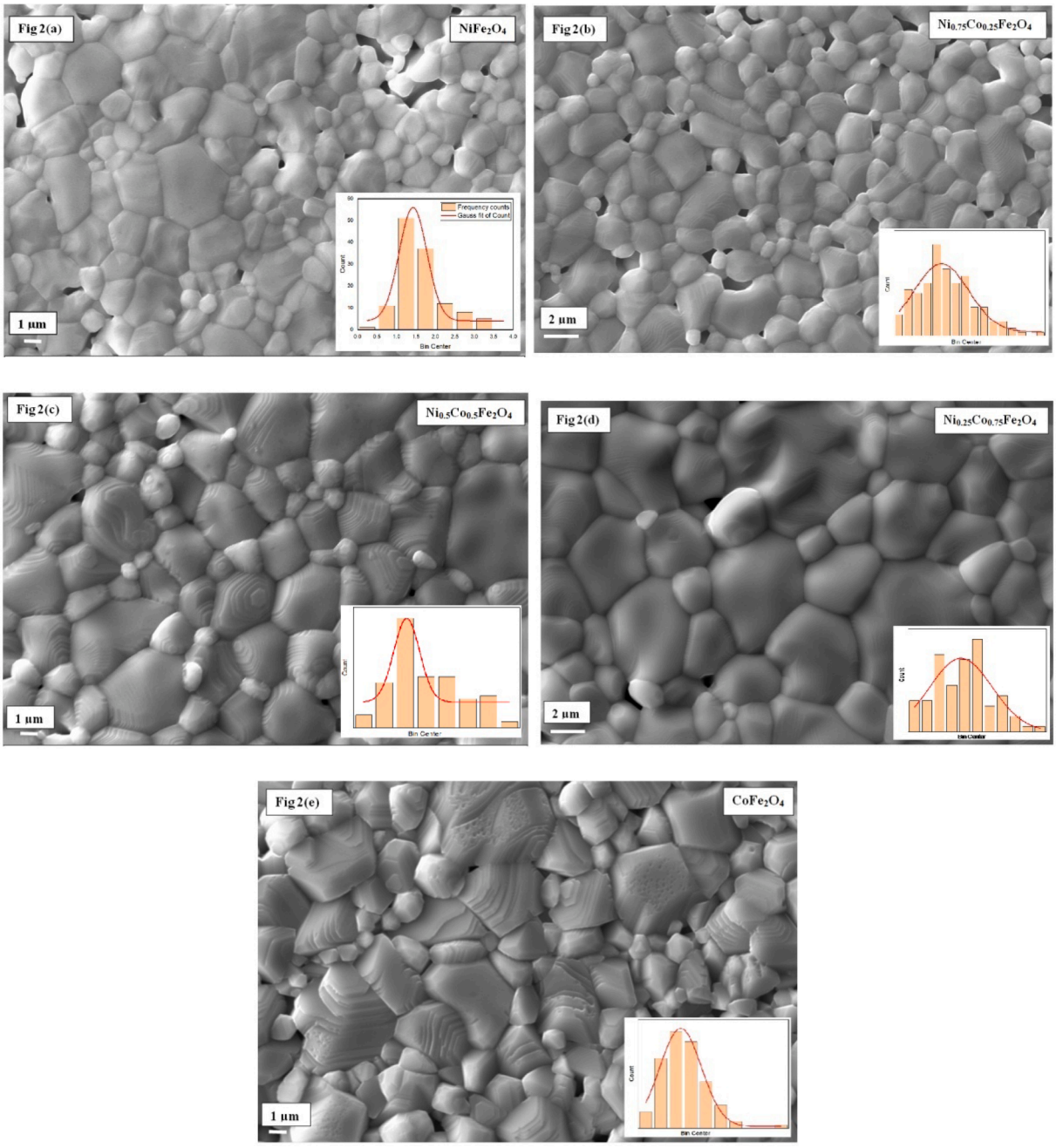


**Fig. 2.** SEM images of $Ni_{1-x}Co_xFe_2O_4$ samples where (a) x = 0, (b) x = 0.25, (c) x = 0.5, (d) x = 0.75 and x = 1 with histograms.

shown in Fig. 1. The sharp peaks indicate the crystalline nature of the samples. The XRD patterns are compared with that of literature [36] and found that the samples are crystallized in a FCC cubic spinel structure with no additional phases. It was observed that there is a slight increase in the lattice parameters with increase of Co substitution. The shift in peaks indicates the expansion of lattice volumes because $Ni^{+2}$ have smaller radii (0.63 Å) than $Co^{+2}$ radii (0.74 Å). The shifting of XRD peaks towards lower angles with the substitution of Co indicates the

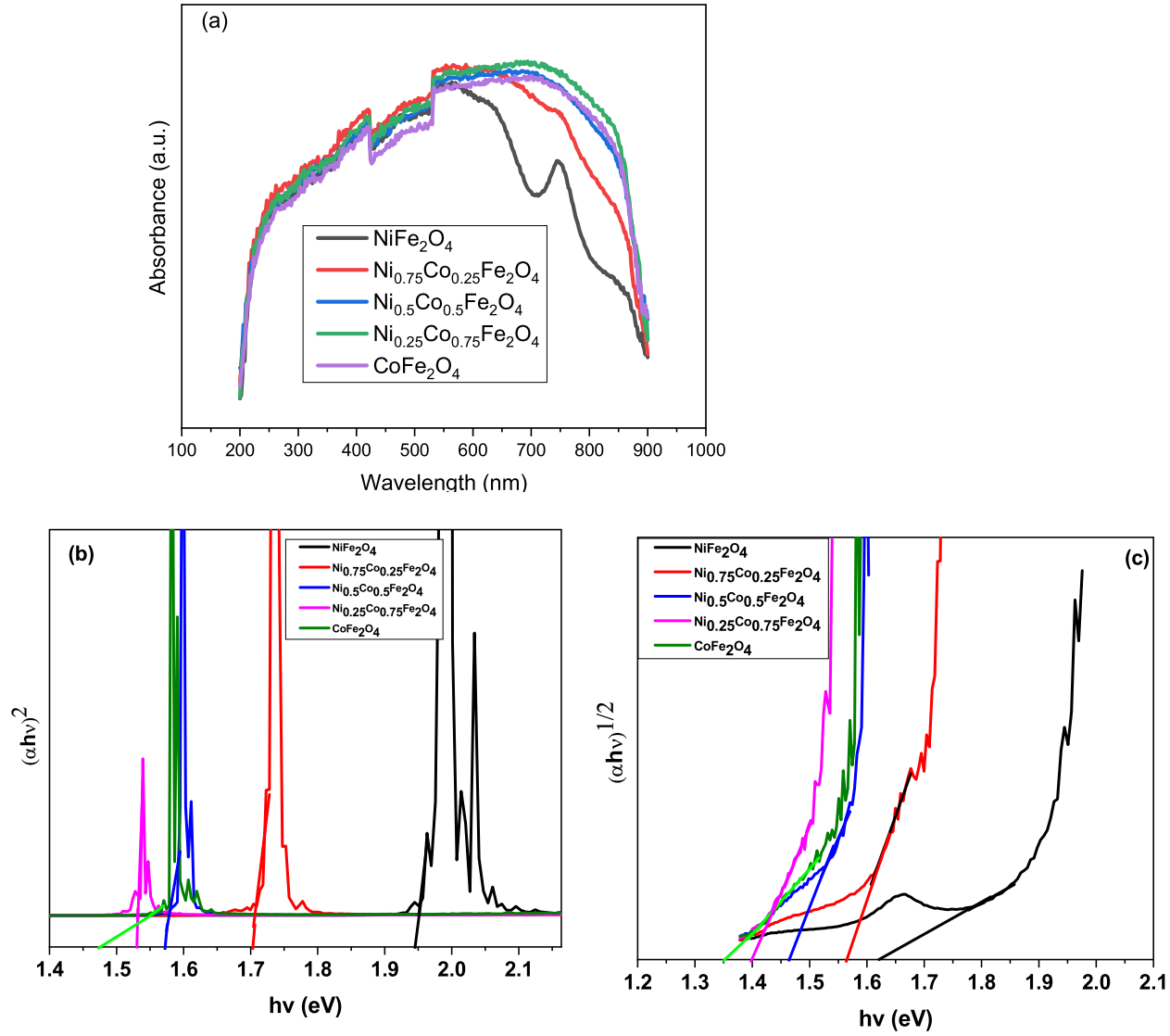


**Fig. 3.** a) Room temperature absorption spectra of Co substituted Ni ferrites. (b&c) The Tauc plots for direct and indirect bandgap for Co substituted Ni ferrites.

migration of $Fe^{+3}$ ions from tetrahedral to octahedral site. The average crystallize sizes for all ferrite samples were determined using the Scherrer formula $D = \frac{0.94\lambda}{\beta cos\theta}$, where λ is the X-ray wavelength (For Cu $K_\alpha$ radiation wavelength is 1.5406 Å), θ is the half of the Bragg diffraction angle for maximum intensity peak, β is the FWHM of the XRD peak of the maximum intensity peak [37]. The average crystallite size was calculated as 69 nm. The crystallite sizes of ferrite samples were shown in Table 1. The variation of crystallite size with cobalt substitution was not systematic; this may be due to the internal micro-strain during the reaction.

The X-ray density for each composition was calculated from the equation $d_x = \frac{ZM}{N_A a^3}$, [38]. Here Z is the number of molecules per unit cell which is 8 for the spinel cubic structure, M is the molecular weight of the corresponding composition, Avagadro's number is $N_A$ and the volume of the unit cell is $a^3$. The values of X-ray density were tabulated in Table 1. The numerical values of X-ray densities decreased from 5.377 to 5.261 $gm/cm^3$. This can be attributed to the increase in molecular weight of composition and decease in volume with Co substitution. Besides, the increase of lattice constant from 8.335 to 8.398 Å with cobalt substitution from x = 0.0 to 1.0 was the important reason for the decrease of the X-ray density.

The distance between magnetic ions (hopping length) in A site (tetrahedral) $L_A = \frac{a\sqrt{3}}{4}$ and B site (octahedral) $L_B = \frac{a\sqrt{2}}{4}$ of ferrites was calculated (where the symbols have their usual meaning) and was listed in Table 1 as a function of 'x'. It was observed that the hopping length increased with the increase of the Co substitution in nickel ferrite system. This is due to the higher ionic radius of $Co^{+2}$ in comparison to $Ni^{+2}$ radius. It was understood from the values that Ni and Co have a very low tendency for A-site occupancy and $Fe^{+3}$ is not equally divided between A and B-sites.

### 3.2. Scanning electron microscopy

Fig. 2 indicates the scanning electron microscope images of Co substituted Ni ferrites which show that ferrites have homogeneous microstructures with micro-grain size, have well-defined edges and were hexagonal and spherical in shape. Also, the doping amounts of $Co^{2+}$ in $Ni_xCo_{1-x}Fe_2O_4$ did not influence the microscopic morphologies attributed to the similarity of atomic size between Ni and Co atoms. The grain size was calculated using ImageJ software and the values were listed in Table 1 for each ferrite. The variation of grain size was not systematic like crystallite size caused due to the internal micro strain during the reaction.

**Table 2**
The direct and indirect band gap values of Co substituted Ni ferrites.

| Name | Direct bandgap (eV) | Indirect bandgap (eV) |
|---|---|---|
| $NiFe_2O_4$ | 1.945 | 1.62 |
| $Ni_{0.75}Co_{0.25}Fe_2O_4$ | 1.7 | 1.565 |
| $Ni_{0.5}Co_{0.5}Fe_2O_4$ | 1.57 | 1.465 |
| $Ni_{0.25}Co_{0.75}Fe_2O_4$ | 1.53 | 1.399 |
| $CoFe_2O_4$ | 1.477 | 1.355 |

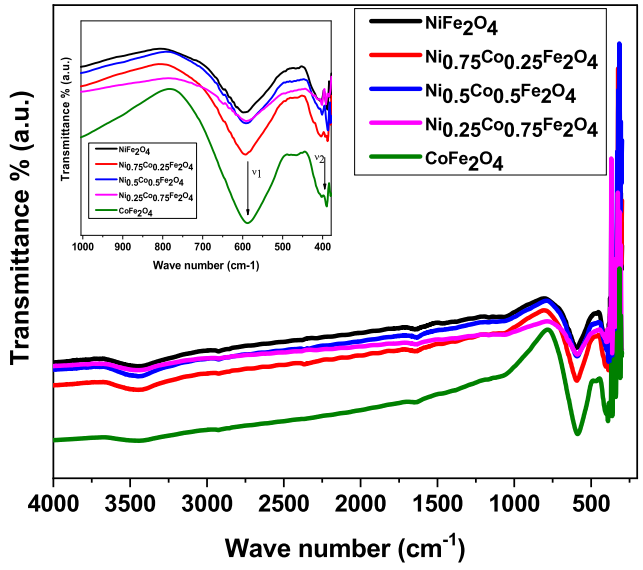


**Fig. 4.** Room temperature FTIR spectra of Co substituted Ni ferrites and inset shows the closed view of $\nu_1$ and $\nu_2$ bands of all ferrites.

### 3.3. Optical properties

#### 3.3.1. UV-DRS

Fig. 3(a) shows the room temperature optical absorption spectra in the wavelength region 200–900 nm. From the figure, it was clear that absorbance was similar in all ferrite samples. It was observed that the absorbance spectra showed humps at around 425, 532, 640 nm for all samples and additional hump at 747 nm in case of pure $NiFe_2O_4$. KubelkaMunk model was used to calculate the bandgaps of ferrite samples. From diffuse reflectance spectra (DRS), the absorption coefficient was found by using the formula $F(R) = \alpha = \frac{(1-R)^2}{2R}$. Here α is absorption coefficient, R is reflectance and F(R) is KubelkaMunk function. The bandgap energy ($E_g$) values were calculated using the formula $h\nu = A(h\nu - E_g)^n$ . Here hν is the energy of the photon and A is the material parameter and n is the transition parameter. n = 2 represents indirect transitions and n=½ represents direct transitions. The direct bandgap energy values were calculated by drawing Tauc plots $(\alpha h\nu)^2$ versus hν and indirect bandgap energy values were calculated by drawing plots $(\alpha h\nu)^{\frac{1}{2}}$ versus hν as shown in Fig. 3(b) and 3(c)[39]. The value of bandgap is calculated from the intercept obtained by extrapolating the linear portion of the graph [40]. The measured energy gap values were given in Table 2. The bandgap values decrease as Co substitution increases [10]. In the $NiFe_2O_4$ inverse spinel structure, the top of the valence band is formed by octahedral Ni d states and the bottom of the conduction band is formed by octahedral Fe d states and tetrahedral Fe d states. When Co is introduced, the introduction of additional tetrahedral d states shifts the valence band up in energy and decreases the band gap.

With the increase of Co concentration, the lattice parameter increases which is directly related to the decrease in bandgap because the energy gap is inversely proportional to interatomic distance. The increase in hopping length with Co tends to change in the concentration of Co in A site hence the additional tetrahedral d states and decrease in bandgap.

#### 3.3.2. FTIR spectroscopy

The room temperature FTIR spectra recorded in the wavenumber range of 4000–200 $cm^{-1}$. Fig. 4 indicates that there were two major bands in the FTIR spectra of spinel ferrites. The band observed around 590 $cm^{-1}$(higher wavenumber $\nu_1$) corresponds to the tetrahedral metal oxygen stretching, $M_{tetra} \leftrightarrow O$. Another band (lower wave number $\nu_2$) observed around 387 $cm^{-1}$ corresponds to octahedral metal oxygen stretching, $M_{octa} \leftrightarrow O$. The band positions result from the difference in the distance of $Fe^{+3}$ - $O^{-2}$ ions associated with the tetrahedral and octahedral complexes. The larger ionic radius of $Co^{+2}$ compared to $Ni^{+2}$ results in a large distance of Fe-O. With the increase of Co substitution, the characteristic band $\nu_1$ shows a shift towards a lower wavenumber region. The values are 597, 594, 592, 590 and 582 $cm^{-1}$ respectively for $Ni_{1-x}Co_xFe_2O_4$ (x = 0, 0.25, 0.5, 0.75 and 1). This may be due to the higher atomic mass of Co compared to Ni because in FTIR spectra the frequency of vibration and wave number were inversely proportional to the mass of the molecule. Hence addition of Co leads to decrease in wavenumber.

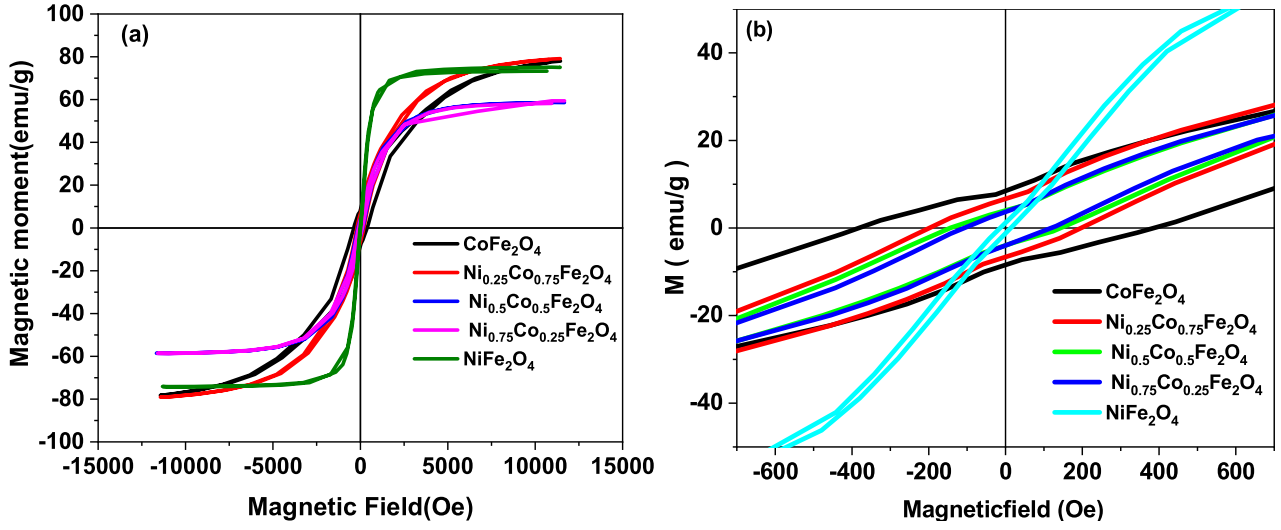


**Fig. 5.** (a) The room temperature magnetic hysteresis loops of Co substituted Ni ferrites, (b) Closed view of loops of samples at the centre.

**Table 3**
The values of saturation magnetization $M_s$, remanent magnetization $M_r$, coercive field $H_c$, Curie temperature ($T_c$), Curie constant (C) and Effective magnetic moment ($\mu_{eff}$) of Co substituted Ni ferrites.

| Sample | $M_s$(emu/g) | $M_r$ (emu/g) | $H_c$ (Oe) | $T_c$ (K) | Curie constant C (emu. K/Oe. mol) | Effective magnetic moment per molecule $\mu_{eff}$ ($\mu_B$) |
|---|---|---|---|---|---|---|
| $NiFe_2O_4$ | 74 | 1 | 10 | 848 | 0.264 | 1.45 |
| $Ni_{0.75}Co_{0.25}Fe_2O_4$ | 58 | 4 | 100 | 856 | 0.355 | 1.68 |
| $Ni_{0.5}Co_{0.5}Fe_2O_4$ | 59 | 5 | 140 | 811 | 0.477 | 1.95 |
| $Ni_{0.25}Co_{0.75}Fe_2O_4$ | 79 | 7 | 200 | 806 | 0.559 | 2.11 |
| $CoFe_2O_4$ | 78 | 9 | 380 | 790 | 1.055 | 2.90 |

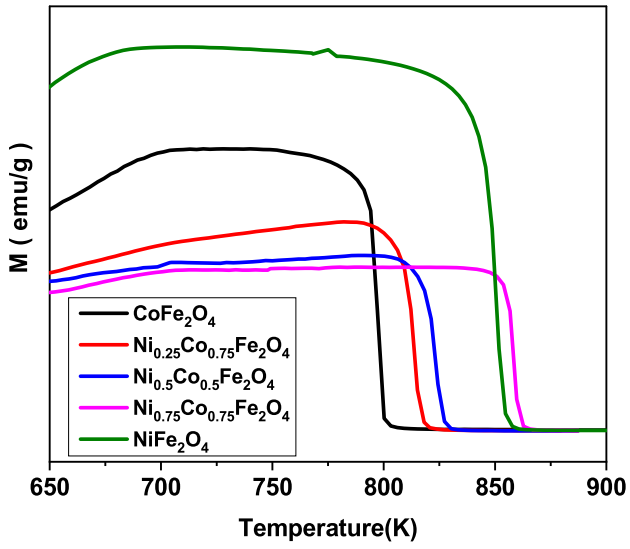


**Fig. 6.** The variation of magnetization with temperature for Co substituted Ni ferrites.

### 3.4. Magnetic properties

#### 3.4.1. M vs H

Fig. 5 M vs H shows the magnetic hysteresis loops of cobalt substituted nickel ferrite samples at room temperature. From the figure, saturation magnetization $M_s$, remanent magnetization $M_r$, coercive field $H_c$ and Curie temperature ($T_c$) were calculated and given in Table 3. $M_r$ and $H_c$ were found to increase with the increase of Co substitution in the Ni ferrite.

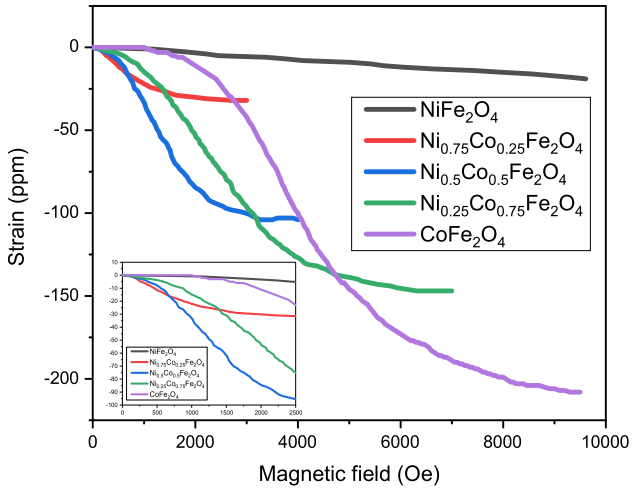


**Fig. 7.** Dependence of strain on magnetic field for Co substituted Ni ferrites; inset shows the closed view of strain at low magnetic fields.

The $M_s$ variation is not uniform with increasing Co concentration. Due to high crystallinity and uniform morphology, $NiFe_2O_4$ shows high $M_s$ and low $H_c$ values [41]. With Co substitution non uniform $M_s$ variation may be due to grain size which leads to variation in surface to volume ratio and also surface defects [42]. The increase of $M_r$, $H_c$ values can be explained by Neel's theory and by the super-exchange interaction. The magnetic moments of the ions in tetrahedral (A) and octahedral (B) are in opposite directions. The spins of electrons of $Fe^{+3}$ in A and B sites were antiparallel to each other and fail to produce a net magnetic moment of $2\mu_B$ due to $Ni^{+2}$ ions at B sites [31]. The substituent $Co^{+2}$, with the magnetic moment of $3\mu_B$, occupy preferably B sites. The increase in $M_r$ originates from the replacement of $Ni^{+2}$ ($2\mu_B$-two unpaired electrons) with $Co^{+2}$ ($3\mu_B$ -three unpaired electrons) that increase the number of unpaired electrons at octahedral sites. As Co concentration increases, the atomic magnetic moment between A and B sites increases and dominates A-O-B super-exchange interaction hence the saturation magnetization increases. A small increase in the $M_r$ with increase in Co substitution was observed which is due to the presence of $Co^{+2}$ ions in the ferrites.

The $H_c$ of a magnetic material is a measure of its magneto crystalline anisotropy. It was found that the $H_c$ was increased with increasing Co content. This behaviour can be attributed to the larger magneto-crystalline anisotropy characteristic to $CoFe_2O_4$. As $Co^{+2}$ has a higher anisotropic character than $Ni^{+2}$, it generates a larger $H_c$, when the Co substitution increases. This is due to the increase of the anisotropy field, which enhances the energy of the magnetic domain wall. By replacing $Ni^{+2}$ with $Co^{+2}$, the ferromagnetic super-exchange interaction is reduced and the antiferromagnetic interaction is strengthened. But replacement of lower magnetic moment $Ni^{+2}$ with higher magnetic moment $Co^{+2}$ would increase $H_c$ and $M_r$ values.

#### 3.4.2. M vs T

Fig. 6 shows the variation of magnetization with temperature. It can be seen from the figure that with decreasing temperature from 900 K, the magnetization of the samples is found to be almost constant (near to zero) up to their Curie temperatures. These low magnetization values represent the paramagnetic nature of the samples. The curie temperatures ($T_c$) of the samples are obtained from the differential curves (dM/dT vs T, not given) of the samples and are given in Table 3. On further decrease from their $T_c$, the magnetization values are increased and saturated. The samples are found to be ferrimagnetic in nature in this region. From Fig. 6 and Table 3, it is clear that the values of $T_c$ of the samples decrease with increasing Co content. According to Neel's theory, the Curie temperature depends on the strength of A-B sublattice interaction of $Fe^{+3}$ ions. As $Co^{+2}$ ions increase, they go to the B site through migration of $Fe^{+3}$ ions from B to A site. The increase in the lattice parameter, bond length results in a decrease in A-B interaction with Co substitution. This causes a gradual decrease to AB interaction and comparatively lesser thermal energy required to disorient the moments leading to a decrease in $T_c$ with the increase of Co substitution [30]. From susceptibility fitting graph $\frac{1}{\chi} = \frac{T-T_c}{C} = \frac{H}{M}$, the curie constant values were measured. From experimental data, the effective magnetic moment values were calculated from the formula $\mu_{eff} = \sqrt{\frac{3CK_B}{N}}$ where C is curie constant, $K_B$ is Boltzmann constant and N is Avagadro number [9,43]. If $M_A$ and $M_B$ are the magnetic moments of A and B ions then the saturation magnetic moment per formula unit at 0K can be calculated by the formula $M = [(1-x)M_A + (1+x)M_B] - [xM_A + (1-x)M_B]$. Theoretical magnetic moment values for nickel ferrite and cobalt ferrite are 2 and 3 $\mu_B$ respectively. The values from experimental data are lower than theoretical values.

**Table 4**

The values of $\lambda_s$, $(\frac{d\lambda}{dH})_{max}$, Field at $(\frac{d\lambda}{dH})_{max}$ and $\lambda_s \times (\frac{d\lambda}{dH})_{max}$ of Co substituted Ni ferrites from magnetostriction graph. Also included the data of previous other articles for reference.

| Sample | $\lambda_s$(ppm) | $(\frac{d\lambda}{dH})_{max}$ ($10^{-9}A^{-1}m$) | Field at $(\frac{d\lambda}{dH})_{max}$(Oe) | $\lambda_s \times (\frac{d\lambda}{dH})_{max}$($10^{-9}A^{-1}m$) | Reference |
|---|---|---|---|---|---|
| $NiFe_2O_4$ | −19 | −0.048 | 2227 | 0.912 | Present study |
| $Ni_{0.75}Co_{0.25}Fe_2O_4$ | –32 | −0.52 | 236 | 16.64 | Present study |
| $Ni_{0.5}Co_{0.5}Fe_2O_4$ | −104 | −1.74 | 1515 | 180.96 | Present study |
| $Ni_{0.25}Co_{0.75}Fe_2O_4$ | −147 | −1.5 | 2081 | 220.5 | Present study |
| $CoFe_2O_4$ | −208 | −1.0 | 3675 | 208 | Present study |
| $CoFe_2O_4$ | −183, 221 | 0.72 | – | – | [44,45] |
| $NiFe_2O_4$ | −35 | – | – | – | [46] |
| $Ni_{0.9}Co_{0.1}Fe_2O_4$ | −36 | 0.6 | 653 | – | [47] |
| $Ni_{0.2}Co_{0.8}Fe_2O_4$ | −45 | – | – | – | [20] |
| $Ni_{0.4}Co_{0.6}Fe_2O_4$ | –33 | – | – | – | [20] |
| $Ni_{0.1}Co_{0.9}Fe_2O_4$ | −115 | – | – | – | [48] |

### 3.5. Magnetostriction

The change in the shape of the material when placed in a magnetic field is known as magnetostriction. In crystal lattices, magnetostrictive property depends on the distance between an individual atom or ion and its nearest neighbor i.e. on the cation distribution between A and B sites of spinel ferrite and also on A-O-B super-exchange between metal ions caused by the overlap between 2p orbital of the $O^{-2}$ ion with 3d orbital of transition metal ions. Substitution of different metal ions (magnetic or non-magnetic) in place of A and B sites in cobalt or nickel ferrite is known to affect the magnetocrystalline anisotropy by perturbing the cation distributions and the A-O-B exchange strength and hence the magnetostriction parameters. Such perturbation in the substituted cobalt ferrite strongly pertains to the valency (di-, tri-, and tetra-valent), amount, size, and the site preference (tetrahedral or octahedral) of the substituted metal ions. Apart from substitution, magnetostriction parameters ferrite samples are also influenced by the synthesis and processing conditions, which are associated with changes in the microstructure [35].

Fig. 7, shows the variation of magnetostriction with applied fields of Co substituted Ni ferrites. The $\lambda_s$, $(\frac{d\lambda}{dH})_{max}$, $\lambda_s \times (\frac{d\lambda}{dH})_{max}$ values were given in Table 4. The negative sign of λ values only indicates the shrinkage along magnetic field direction. From Fig. 7 the magnetostriction (λ in ppm) of $NiFe_2O_4$ is ∼−20 at 10 KOe and the value of λ with applied field increases with Co substitution. This behaviour is due to an increase in magnetic anisotropy with Co substitution in $NiFe_2O_4$ [3]. $CoFe_2O_4$ shows a significant increase of the property compared to other ferrites at higher fields. For $CoFe_2O_4$, λ is ∼−200 ppm at 10 KOe. But $Ni_{0.5}Co_{0.5}Fe_2O_4$ shows a good magnetostriction value even at low magnetic fields i.e. ∼−63 at 1500 Oe and ∼−85 at 2000 Oe. Though $CoFe_2O_4$ has a high λ value, $Ni_{0.5}Co_{0.5}Fe_2O_4$ is showing better values at lower fields. In crystalline $Ni_{1-x}Co_xFe_2O_4$ samples, the distance between the cations in pure Ni and Co ferrites is the same. Hence at lower external magnetic fields, these two samples were showing less magnetostriction as there is less scope for change in distance between two cations. But in the case of Ni-Co ferrites, as both the ions exist at the same site, the distance between $Ni^{+2}$ and $Co^{+2}$ ions are not constant. It varies with composition and nearest neighboring atoms. Hence even at low fields, there is a possibility to change the distance between cations thereby magnetostriction values are higher in Ni-Co ferrites compared to pure ferrites.

The very low magnetostriction values of around −10 ppm at 1500 Oe for Ni-Co ferrites were reported by co-precipitation method. Even at 3000 Oe, the λ values for $Ni_{1-x}Co_xFe_2O_4$ (x = 0, 0.2, 0.4, 0.6, 0,8 and 1) were −7, −12, –22, −28 and –32 ppm respectively which were very low and increasing with Co substitution [20]. But in the present study it was found that even at low magnetic fields these samples were showing high λ and strain sensitivity values. From closed view of Fig. 7, it was clear that at 1500 Oe, $Ni_{1-x}Co_xFe_2O_4$ (x = 0, 0.25, 0.5, 0.75 and 1) have the λ values −2, −28, −63, −30 and −4ppm respectively.

Piezomagnetic coefficient $\frac{d\lambda}{dH}$ determines the strain sensitivity of the magnetic material. $(\frac{d\lambda}{dH})_{max}$ values (The curves are not given) increased with Co substitution and reached maximum for $Ni_{0.5}Co_{0.5}Fe_2O_4$ and then decreased. Higher strain sensitivity of the substituted ferrites may be due to the reduction in magnetic anisotropy and A-O-B super exchange interaction which depends on the distribution of substituted metal ions. From Table 4, it is clear that strain sensitivity is higher i.e. $1.74x10^{-9}A^{-1}m$ for $Ni_{0.5}Co_{0.5}Fe_2O_4$ even at low fields (∼1500 Oe) in comparison with other ferrites.

With the substitution of Co the strain sensitivity (dλ/dH) was found to increase upto x = 0.5 and with subsequent increase in Co content dλ/dH was found to decrease. $NiFe_2O_4$ has low anisotropy and accordingly, the magnetostriction and saturation field for achieving saturation magnetostriction was low. However, with increase in Co content, the increase in the magnetic anisotropy due to the perturbation in the cation distribution was found to increase the magnetostriction. In addition to this the field required for saturating the magnetic domains was also higher and hence saturation occured at higher field.

Magnetostriction (λ) and strain sensitivity $(\frac{d\lambda}{dH})_{max}$ were the two important parameters of the magnetostrictive materials for contactless torque sensing applications which in turn was useful for ME energy harvesting applications. As $Ni_{0.5}Co_{0.5}Fe_2O_4$ was showing better magnetostriction and strain sensitivity values at lower magnetic fields compared to other ferrites, it can be used as a piezomagnetic material in ME energy harvesting applications.

## 4. Conclusions

The series of cobalt substituted nickel ferrites with compositional formula $Ni_{1-x}Co_xFe_2O_4$ (x = 0, 0.25, 0.5, 0.75 and 1) were successfully synthesized by sol–gel technique and found to possess cubic spinel structure. The systematic change in the M−O bands with Co substitution in nickel ferrite samples was observed in FTIR spectra. The coercivity exhibited an increasing trend upon Co substitution owing to the increase in the magnetic anisotropy with Co addition. Further, increase in magnetic anisotropy also manifested in the magnetostriction values which exhibited a considerable improvement with the addition of Co. The compound $Ni_{0.5}Co_{0.5}Fe_2O_4$ showed higher strain sensitivity at low magnetic field making it a potential candidate for magnetic actuator and transducer applications.

## Declaration of Competing Interest

The authors declare that they have no known competing financial interests or personal relationships that could have appeared to influence the work reported in this paper.

**Acknowledgements:**

The authors are thankful to Dr.A.Srinivas, Scientist F, DMRL, Hyderabad for initiation and support to do this work. The authors are thankful to Dr.Partha Ghoshal, Scientist G, DMRL, Hyderabad for the SEM images and to Prof.M.Vittal(Retd.), Department of Chemistry, Osmania University, Hyderabad for the XRD measurements.The authors are also thankful to Head of the Department of Physics, Osmania University for providing experimental facilities. The author P.Sowjanya is thankful to Dr.P.V.Umasasi, Principal, GDC(W), Gajwel, Telangana for her constant support in this work.

## References

[1] F. Narita, M. Fox, A review on piezoelectric, magnetostrictive, and magnetoelectric materials and device technologies for energy harvesting applications, Adv. Eng. Mater. 20 (5) (2018) 1–22, https://doi.org/10.1002/adem.201700743.
[2] C.P. Poole, H.A. Farach, R.J. Creswick, R. Prozorov, Transport properties, Superconductivity 2 (2) (2007) 489–529, https://doi.org/10.1016/b978-012088761-3/50038-7.
[3] M. Atif, M. Nadeem, R. Grössinger, R.S. Turtelli, Studies on the magnetic, magnetostrictive and electrical properties of sol-gel synthesized Zn doped nickel ferrite, J. Alloys Compd. 509 (18) (2011) 5720–5724, https://doi.org/10.1016/j.jallcom.2011.02.163.
[4] K. Kamala Bharathi, J. Arout Chelvane, G. Markandeyulu, Magnetoelectric properties of Gd and Nd-doped nickel ferrite, J. Magn. Magn. Mater. 321 (22) (2009) 3677–3680, https://doi.org/10.1016/j.jmmm.2009.07.011.
[5] K.K. Bharathi, G. Markandeyulu, C.V Ramana, Structural, magnetic, electrical, and magnetoelectric properties of Sm- and Ho-substituted, pp. 554–560, 2011.
[6] A.B. Nawale, N.S. Kanhe, S.A. Raut, S.V. Bhoraskar, A.K. Das, V.L. Mathe, Investigation of structural, optical and magnetic properties of thermal plasma synthesized Ni-Co spinel ferrite nanoparticles, Ceram. Int. 43 (9) (2017) 6637–6647, https://doi.org/10.1016/j.ceramint.2017.02.022.
[7] D.M. Ghone, V.L. Mathe, K.K. Patankar, S.D. Kaushik, Microstructure, lattice strain, magnetic and magnetostriction properties of holmium substituted cobalt ferrites obtained by co-precipitation method, J. Alloys Compd. 739 (2018) 52–61, https://doi.org/10.1016/j.jallcom.2017.12.219.
[8] S.R. Naik, A.V. Salker, Change in the magnetostructural properties of rare earth doped cobalt ferrites relative to the magnetic anisotropy, J. Mater. Chem. 22 (6) (2012) 2740–2750, https://doi.org/10.1039/c2jm15228b.
[9] D.C. Jiles, N. Bowler, R.J. Weber, Magnetic and magnetoelastic properties of M-substituted cobalt ferrites (M=Mn, Cr, Ga, Ge) by Sang-Hoon Song A, 2007.
[10] K. Dileep, B. Loukya, N. Pachauri, A. Gupta, R. Datta, Probing optical band gaps at the nanoscale in NiFe2O4 and CoFe2O4 epitaxial films by high resolution electron energy loss spectroscopy, J. Appl. Phys. 116 (10) (2014), https://doi.org/10.1063/1.4895059.
[11] R.M. Bozorth, J.G. Walker, Magnetostriction of single crystals of cobalt and nickel ferrites [12], Phys. Rev. 88 (5) (1952) 1209, doi: 10.1103/PhysRev.88.1209.
[12] A.B. Smith, R.V. Jones, Magnetostriction in nickel ferrite and cobalt - nickel ferrite, J. Appl. Phys. 37 (3) (1966) 1001–1002, https://doi.org/10.1063/1.1708305.
[13] A.A. Ati, Z. Othaman, A. Samavati, Influence of cobalt on structural and magnetic properties of nickel ferrite nanoparticles, J. Mol. Struct. 1052 (2013) 177–182, https://doi.org/10.1016/j.molstruc.2013.08.040.
[14] K. Pubby, K. Vijay Babu, S. Bindra Narang, Magnetic, elastic, dielectric, microwave absorption and optical characterization of cobalt-substituted nickel spinel ferrites, Mater. Sci. Eng. B Solid-State Mater. Adv. Technol. 255 (2020) 114513, https://doi.org/10.1016/j.mseb.2020.114513.
[15] X. Chen, C. Hou, Q. Zhang, Y. Li, H. Wang, One-step synthesis of Co-Ni ferrite/graphene nanocomposites with controllable magnetic and electrical properties, Mater. Sci. Eng. B Solid-State Mater. Adv. Technol. 177 (13) (2012) 1067–1072, https://doi.org/10.1016/j.mseb.2012.05.001.
[16] A.A. Ati, Fast synthesis, structural, morphology with enhanced magnetic properties of cobalt doped nickel ferrite nanoscale, J. Mater. Sci. Mater. Electron. 29 (14) (2018) 12010–12021, https://doi.org/10.1007/s10854-018-9305-8.
[17] A. Baykal, N. Kasapoğlu, Y. Köseoğlu, A.C. Başaran, H. Kavas, M.S. Toprak, Microwave-induced combustion synthesis and characterization of Ni x Co 1–x Fe 2 O 4 nanocrystals (x = 0.0, 0.4, 0.6, 0.8, 1.0), Cent. Eur. J. Chem. 6 (1) (2008) 125–130, https://doi.org/10.2478/s11532-007-0070-4.
[18] R.C. Kambale, P.A. Shaikh, S.S. Kamble, Y.D. Kolekar, Effect of cobalt substitution on structural, magnetic and electric properties of nickel ferrite, J. Alloys Compd. 478 (1–2) (2009) 599–603, https://doi.org/10.1016/j.jallcom.2008.11.101.
[19] K. Maaz, W. Khalid, A. Mumtaz, S.K. Hasanain, J. Liu, J.L. Duan, Magnetic characterization of Co1-xNixFe2O4 (0≤x≤1) nanoparticles prepared by co-precipitation route, Phys. E Low-Dimensional Syst. Nanostruct. 41 (4) (2009) 593–599, https://doi.org/10.1016/j.physe.2008.10.009.
[20] V.L. Mathe, A.D. Sheikh, Magnetostrictive properties of nanocrystalline CoNi ferrites, Phys. B Condens. Matter 405 (17) (2010) 3594–3598, https://doi.org/10.1016/j.physb.2010.05.047.
[21] R.S. Melo, P. Banerjee, A. Franco, Hydrothermal synthesis of nickel doped cobalt ferrite nanoparticles: optical and magnetic properties, J. Mater. Sci. Mater. Electron. 29 (17) (2018) 14657–14667, https://doi.org/10.1007/s10854-018-9602-2.
[22] N.B. Velhal, N.D. Patil, A.R. Shelke, N.G. Deshpande, V.R. Puri, Structural, dielectric and magnetic properties of nickel substituted cobalt ferrite nanoparticles: effect of nickel concentration, AIP Adv. 5 (9) (2015) 097166, https://doi.org/10.1063/1.4931908.
[23] F. Tudorache, P.D. Popa, M. Dobromir, F. Iacomi, Studies on the structure and gas sensing properties of nickel-cobalt ferrite thin films prepared by spin coating, Mater. Sci. Eng. B Solid-State Mater. Adv. Technol. 178 (19) (2013) 1334–1338, https://doi.org/10.1016/j.mseb.2013.03.019.
[24] S. Chakrabarty, A. Dutta, M. Pal, Enhanced magnetic properties of doped cobalt ferrite nanoparticles by virtue of cation distribution, J. Alloys Compd. 625 (2015) 216–223, https://doi.org/10.1016/j.jallcom.2014.10.179.
[25] C. Kumari, H.K. Dubey, F. Naaz, P. Lahiri, Structural and optical properties of nanosized Co substituted Ni ferrites by coprecipitation method, Phase Transitions 93 (2) (2020) 207–216, https://doi.org/10.1080/01411594.2019.1709120.
[26] M. Sedlar, I. Paulicka, M. Sayer, Optical fiber magnetic field sensors with ceramic magnetostrictive jackets, Appl. Opt. 35 (27) (1996) 5340, https://doi.org/10.1364/ao.35.005340.
[27] Z.M. Abdulhamid, A.A. Sattar, A.S. Darwish, A.A. Ghani, Dependence of the magnetic and optical properties of Ni-Co nanoferrite on the particle shape, J. Phys.: Conf. Ser. 1253 (1) (2019) 012022, https://doi.org/10.1088/1742-6596/1253/1/012022.
[28] Z.M. Abdulhamid, A.A. Sattar, A.S. Darwish, A.A. Ghani, Correlation of cation distribution with structure, magnetic and electrical properties of ultrafine Ni2+-doped CoFe2O4, Appl. Phys. A 126 (10) (2020), https://doi.org/10.1007/s00339-020-03997-2.
[29] Z.M. Abdulhamid, A.A. Sattar, A.S. Darwish, A.A. Ghani, Impact of nanorod morphology on microstructure, magnetic and electrical properties of NixCo1-xFe2O4, Phys. B Condens. Matter 601 (November 2020) (2021) 412585, doi: 10.1016/j.physb.2020.412585.
[30] K.K. Bestha, J.J. Abraham, J.A. Chelvane, V. Gorige, Influence of cation distribution on magnetic response of polycrystalline Co1-xNixFe2O4(0 ≤ x ≤ 1) ferrites, Phys. Scr. 95 (8) (2020), doi: 10.1088/1402-4896/aba3d2.
[31] T. Dippong, E.A. Levei, O. Cadar, I.G. Deac, L. Diamandescu, L. Barbu-Tudoran, Effect of nickel content on structural, morphological and magnetic properties of NixCo1-xFe2O4/SiO2 nanocomposites, J. Alloys Compd. 786 (2019) 330–340, https://doi.org/10.1016/j.jallcom.2019.01.363.
[32] M.R. De Freitas, G.L. De Gouveia, L.J.D. Costa, A.J.A. De Oliveira, R.H.G. A. Kiminami, Microwave assisted combustion synthesis and characterization of nanocrystalline nickel-doped cobalt ferrites, Mater. Res. 19 (2016) 27–32, https://doi.org/10.1590/1980-5373-MR-2016-0077.
[33] K.M. Srinivasamurthy, J. Angadi V, S.P. Kubrin, S. Matteppanavar, D.A. Sarychev, P.M. Kumar, H.W. Azale, B. Rudraswamy, Tuning of ferrimagnetic nature and hyperfine interaction of Ni2+ doped cobalt ferrite nanoparticles for power transformer applications, Ceram. Int. 44 (8) (2018) 9194–9203, https://doi.org/10.1016/j.ceramint.2018.02.129.
[34] U.B. Sontu, N.R. G, F.C. Chou, V.R.R. M, Temperature dependent and applied field strength dependent magnetic study of cobalt nickel ferrite nano particles: synthesized by an environmentally benign method, J. Magn. Magn. Mater. 452 (2018) 398–406, https://doi.org/10.1016/j.jmmm.2018.01.003.
[35] P.N. Anantharamaiah, P.A. Joy, Tuning of the magnetostrictive properties of cobalt ferrite by forced distribution of substituted divalent metal ions at different crystallographic sites, J. Appl. Phys. 121 (9) (2017) 093904, https://doi.org/10.1063/1.4977758.
[36] A. Kumar, P. Sharma, D. Varshney, Structural, vibrational and dielectric study of Ni doped spinel Co ferrites: Co1−xNixFe2O4 (x=0.0, 0.5, 1.0), Ceram. Int. 40 (8) (2014) 12855–12860.
[37] T. Joseph, D. Pamu, Structural and magnetic properties of zinc substituted Co 0.8 Mn 0.2 Fe 2 O 4 nanoparticles, AIP Conf. Proc. 1665 (2015) 2–7, https://doi.org/10.1063/1.4917827.
[38] D.R. Kumar, C.A. Lincoln, D. Ravinder, S.I. Ahmad, Structural, morphological, luminescence, magnetic, and electrical transport properties of zinc-doped MnFe2O4 nanomaterials, Appl. Phys. A 126 (9) (2020), https://doi.org/10.1007/s00339-020-03894-8.
[39] J.-L. Ortiz-Quiñonez, U. Pal, M.S. Villanueva, Structural, magnetic, and catalytic evaluation of spinel Co, Ni, and Co-Ni ferrite nanoparticles fabricated by low-temperature solution combustion process, ACS Omega 3 (11) (2018) 14986–15001, https://doi.org/10.1021/acsomega.8b02229.
[40] A. Bieńkowski, R. Szewczyk, Magnetostrictive properties of Mn0.70Zn0.24Fe2.06O4 ferrite, Materials (Basel) 11 (10) (2018) 2–8, https://doi.org/10.3390/ma11101894.
[41] T. Dippong, E.A. Levei, Chapter III Synthesis and characterization of MFe 2 O 4 (M : Zn, Ca, Mg) photocatalysts, 4 (2021) 1–12.
[42] T. Dippong, E.A. Levei, I.G. Deac, E. Neag, O. Cadar, Influence of CU2+, NI2+, and ZN2+ ions doping on the structure, morphology, and magnetic properties of co-ferrite embedded in SiO2 matrix obtained by an innovative sol-gel route, Nanomaterials 10 (3) (2020), doi: 10.3390/nano10030580.
[43] J. Massoudi, M. Smari, K. Nouri, E. Dhahri, K. Khirouni, S. Bertaina, L. Bessais, E. K. Hlil, Magnetic and spectroscopic properties of Ni-Zn-Al ferrite spinel: from the nanoscale to microscale, RSC Adv. 10 (57) (2020) 34556–34580.
[44] N. Somaiah, T.V. Jayaraman, P.A. Joy, D. Das, Magnetic and magnetoelastic properties of Zn-doped cobalt-ferrites - CoFe 2-xZn xO 4 (x=0, 0.1, 0.2, and 0.3), J. Magn. Magn. Mater. 324 (14) (2012) 2286–2291, https://doi.org/10.1016/j.jmmm.2012.02.116.
[45] P.N. Anantharamaiah, P.A. Joy, Enhancing the strain sensitivity of CoFe2O4 at low magnetic fields without affecting the magnetostriction coefficient by substitution

of small amounts of Mg for Fe, Phys. Chem. Chem. Phys. 18 (15) (2016) 10516–10527, https://doi.org/10.1039/c6cp00369a.
[46] A. Aubert, V. Loyau, F. Mazaleyrat, M. LoBue, Investigation of piezomagnetism in nickel ferrite, IEEE Trans. Magn. 57 (6) (2021) 1–5.
[47] M.S. Hieda, J.P.B. Machado, E.d.O. Silva Júnior, M.B.d.S. Dias, C.B. Nunes, R.G.A. d. Lima, A.C.d.C. Migliano, V.L.O.d. Brito, Mechanical, magnetic, and microstructural characterization of Ni0.9Co0.1Fe2O4 produced by the ceramic method, Mater. Res. 21 (3) (2018).
[48] M.M. Sutar, A.N. Patil, Magnetic characterization and instrumentation setup for measurement of co-efficient of magnetostriction on Co0.9Ni0.1Fe2-xMnxO4 ferrite, Mater. Today Proc. 2 (4–5) (2015) 1494–1501, https://doi.org/10.1016/j.matpr.2015.07.075.

Two Day National Conference on

# RECENT INNOVATIONS IN SMART/ NANO MATERIALS

## NCRISNM-2022

On 29th & 30th April, 2022

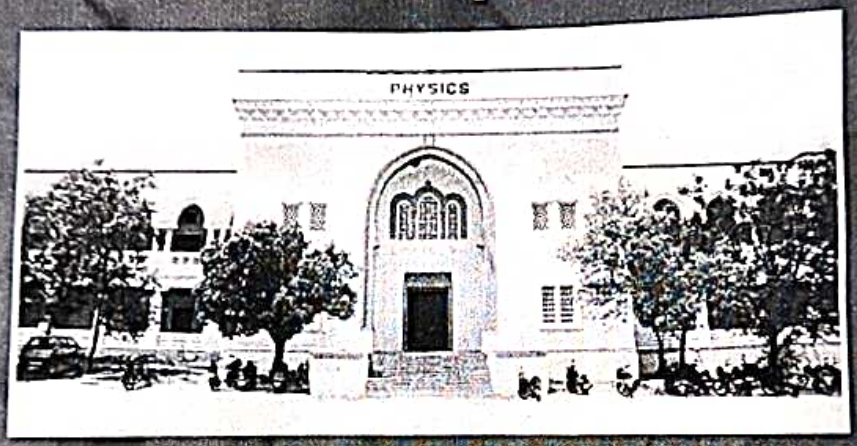


organized under OU & TSCHE

## DEPARTMENT OF PHYSICS

University College of Science,
Osmania University

# SYNTHESIS, STRUCTURAL AND MAGNETIC PROPERTIES OF Ni-Co FERRITES FOR ENERGY HARVESTING APPLICATIONS

B. Brahmanandam[1,2], J. Uma[1], P. Sowjanya[1,3], N. Pavan Kumar[4]

[1]Department of Physics, Osmania University, Hyderabad, Telangana, India
[2]Department of Sciences and Humanities, Vignan Engineering College, Hyderabad, Telangana, India
[3]Department of Physics, Government Degree College for Women, Gajwel, Telangana, India
[4]Corresponding Author Email ID: pavanphysics@gmail.com

**Abstract:**

Ferrites are usually ferrimagnetic ceramic compounds derived from iron oxides. There are ceramic-like materials with magnetic properties, which are used in many types of electronic devices. Nickel Ferrite is a soft ferrite with low magnetostriction where as $CoFe_2O_4$ is a hard ferrite with high magnetostriction. In the present work $Ni_{0.5}Co_{0.5}Fe_2O_4$ sample has been prepared through sol-gel method and sintered at 1200 C for 4 hours. The structure of the sample has been found to be cubic Spinel structure and the lattice parameters are evaluated. The surface morphology of the sample has been studied by using scanning electron microscope. Room temperature and high temperature magnetic properties were studied. Finally, magnetostriction of the sample for the energy harvesting applications have been done and found the higher strain sensitivities at low magnetic field making it a suitable sample for magnetoelectric energy harvesting applications.

| | | | |
|---|---|---|---|
| | SMART TEXTILE<br>Mabelagua A Haque, Zena Joseph, Mrunal Gandole, Subhash B Kondawar | | |
| 31 | ANTIBACTERIAL AND ANTIFUNGAL STUDIES OF SILVER NANOPARTICLES FROM OCIMUM BASILICUM L. VAR. BASILICUM AND OCIMUM BASILICUM L. VAR. THYRSIFLORUM<br>Dr. T. Sujatha, R Shyamala Chandra, B. Srinivas, Anuradha, G | 31 | Oral |
| 32 | GUM KARAYA - A NOVEL POTENTIAL POLYMER IN SMART NANOPARTICLE SYNTHESIS.<br>Shyamala Chandra Rokkala, Sashidhar Rao Beedu and Kamma Rupula | 32 | Poster |
| 33 | GREEN SYNTHESIS OF INDIUM ZINC OXIDE AND ANTIBACTERIAL ACTIVITIES<br>B Shanti Sree, Y Aparna, B Srinivasa Rao, Kanchana Latha Chintha | 33 | Oral |
| 34 | SYNTHESIS, STRUCTURAL AND MAGNETIC PROPERTIES OF Ni-Co FERRITES FOR ENERGY HARVESTING APPLICATIONS<br>B Brahmanandam, J. Uma, P. Sowjanya, N. Pavan Kumar, | 34 | Poster |
| 35 | $Cu_2BiS_3$ THIN FILM BASED METAL-SEMICONDUCTOR-METAL NEAR INFRARED PHOTODETECTOR<br>Reddivari Venugopal, Dr Ch Srinivas | 35 | Oral |
| 36 | STUDIES ON RARE-EARTH DOPED NANO-STRUCTURED CERIA BASED ELECTROLYTES.<br>Ch. Sameera Devi and G. Prasad | 36 | Oral |
| 37 | STUDY OF PHOTO CATALYTICAL, ANTIMICROBIAL ACTIVITY, DIELECTRIC AND AC IMPEDANCE PROPERTIES OF Zn DOPED Mg NANO FERRITES SYNTHESIZED FROM CITRATE GEL AUTO COMBUSTION METHOD<br>D. Ravi Kumar, Ch. Abraham Lincoln, D. Ravinder, M. Veeraswamy | 37 | Poster |
| 38. | PREPARATION AND LUMINESCENCE PROPERTIES OF CERIUM ACTIVATED $Sr_2SiO_4$ PHOSPHOR.<br>Lavudi Narsimha, Konetu Srikanth, Kunja Laxminarayana, Mungili Narsimulu, Amarapuri Trinadh, Manchoju Satish Kumar and Mudavat Srinivas | 38 | Poster |
| 39. | STRUCTURAL, PHOTOCATALYTIC, ELECTROMAGNETIC PROPERTIES OF RARE EARTH METAL Gd DOPED Mg NANO FERRITES SYNTHESIZED BY CITRATE GEL AUTO COMBUSTION METHOD<br>Nakirekanti Venumesh, Shyamsunder Goud, N. Hari | 39 | Poster |